

RESEARCH ARTICLE | MAY 20 2024

Ultra-flat bands at large twist angles in group-V twisted bilayer materials

Zhi-Xiong Que  ; Shu-Zong Li  ; Bo Huang  ; Zhi-Xiong Yang  ; Wei-Bing Zhang  

 Check for updates

J. Chem. Phys. 160, 194710 (2024)
<https://doi.org/10.1063/5.0197757>



APL Energy
Latest Articles Online!

Read Now

AIP Publishing

Ultra-flat bands at large twist angles in group-V twisted bilayer materials

Cite as: J. Chem. Phys. 160, 194710 (2024); doi: 10.1063/5.0197757

Submitted: 14 January 2024 • Accepted: 1 May 2024 •

Published Online: 20 May 2024



View Online



Export Citation



CrossMark

Zhi-Xiong Que, Shu-Zong Li, Bo Huang, Zhi-Xiong Yang, and Wei-Bing Zhang^{a)}

AFFILIATIONS

Hunan Provincial Key Laboratory of Flexible Electronic Materials Genome Engineering, School of Physics and Electronic Sciences, Changsha University of Science and Technology, Changsha 410114, China

^{a)}Author to whom correspondence should be addressed: zhangwbt@csust.edu.cn

ABSTRACT

Flat bands in 2D twisted materials are key to the realization of correlation-related exotic phenomena. However, a flat band often was achieved in the large system with a very small twist angle, which enormously increases the computational and experimental complexity. In this work, we proposed group-V twisted bilayer materials, including P, As, and Sb in the β phase with large twist angles. The band structure of twisted bilayer materials up to 2524 atoms has been investigated by a deep learning method DeepH, which significantly reduces the computational time. Our results show that the bandgap and the flat bandwidth of twisted bilayer β -P, β -As, and β -Sb reduce gradually with the decreasing of twist angle, and the ultra-flat band with bandwidth approaching 0 eV is achieved. Interestingly, we found that a twist angle of 9.43° is sufficient to achieve the band flatness for β -As comparable to that of twist bilayer graphene at the magic angle of 1.08° . Moreover, we also find that the bandgap reduces with decreasing interlayer distance while the flat band is still preserved, which suggests interlayer distance as an effective routine to tune the bandgap of flat band systems. Our research provides a feasible platform for exploring physical phenomena related to flat bands in twisted layered 2D materials.

Published under an exclusive license by AIP Publishing. <https://doi.org/10.1063/5.0197757>

Twisted bilayer materials, which can be formed by combining bilayers of two-dimensional (2D) materials with a twist angle or two different 2D materials with a small lattice mismatch,^{1–3} have attracted great interest recently.^{4–9} It was discovered that flat bands can appear in 2D twisted bilayer materials and lead to exotic physics such as correlated insulating and unconventional superconducting states.^{10,11} Flat bands mean that a large number of quantum states have similar kinetic energies, which will lead to significantly increased electron correlation.^{10,12–14} So far, flat bands have been found in many twisted bilayer 2D materials. For example, a bandwidth of 12 meV has been achieved at a magic angle of 1.08° in twisted bilayer graphene.^{10,11} For other systems, such as transition metal dichalcogenides (TMDCs),^{15–18} hexagonal boron nitride (hBN),¹⁹ and black phosphene,²⁰ similar bandwidths also require very small twist angles of about 2° . The small twist angle means that the twisted bilayer contains a large number of atoms, which increases the investigation complexity. It is thus interesting to explore the flat band with a large twist angle and a small number of atoms.

2D group-V elemental materials, including P, As, and Sb, have attracted extensive attention due to their interesting properties,

such as high carrier mobility and topologically nontrivial states.^{21–26} Among possible 2D allotropes,²⁷ β -phase monolayer has a graphene-like buckled honeycomb structure and excellent stability,^{21–23} which may form an exotic twisted bilayer structure. The detailed knowledge of band structure especially the electronic states near the Fermi level is essential to understand the interesting physical phenomena associated with strong electronic correlations.^{28–30} To date, the band structures of the β -P, β -As, and β -Sb twisted systems have also been explored by density functional theory (DFT) methods.^{31–34} An *et al.* found that the flat bandwidth of 10 meV in β -Sb appeared at 6.01° .³⁴ Agnihotri *et al.* studied the evolution of interlayer coupling in twisted bilayers of β -P and β -As, resulting in significant changes in the bandgap.³¹ However, due to limited computational resources, investigations have been limited to the small system with an angle of 3.89° and 868 atoms. Larger systems with thousands of atoms remain largely unexplored.

Fortunately, recent development of deep learning methods has shown promise in addressing the efficiency and accuracy limit of density functional theory (DFT) calculations.^{35,36} Especially, a deep learning method called DeepH can efficiently and accurately

predict material properties for varying twist angles by training solely on density functional theory data for non-twisted systems.^{37,38} For the calculation of large systems, researchers have recently used real-space KS-DFT methods to achieve electronic structure calculations for systems with thousands of atoms.^{20,39} In contrast, DeepH can directly predict its DFT Hamiltonian based on the information of crystal structure, thus skipping the time-consuming self-consistent iteration process. After post-processing, electronic structure properties such as band structures can be obtained. This approach greatly speeds up electronic structure calculations and opens new possibilities for studying large twisted bilayer systems. In this paper, we have investigated the electronic structure of twisted β -P, β -As, and β -Sb bilayer at smaller twist angles by using the DeepH method and found that the flat bandwidth is less than 10 meV at a large twist angle.

All DFT calculation and geometry optimization are performed using Vienna *ab initio* simulation package (VASP) code⁴⁰ within the projector augmented-wave (PAW) method.^{41,42} The generalized gradient approximation (GGA) in the form of Perdew–Burke–Ernzerhof (PBE) has been used.⁴³ The energy cutoff of the plane-wave expansion was set to 400 eV and a k-mesh of $15 \times 15 \times 1$ according to the Monckhorst–Pack scheme is adopted to sample the Brillouin zone (BZ). To consider interlayer van der Waals (vdW) interactions, the DFT-D3 method with Becke–Jonson damping was used.^{44,45} All atoms were allowed to relax until the Hermann–Feynman force of each atom was less than 0.015 eV/Å. A large vacuum larger than 20 Å was set to eliminate artificial interactions in adjacent unit cells. Spin–orbit coupling (SOC) was not included in the structural optimization.

To train DeepH models for twisted bilayer materials, we prepared datasets for β -P, β -As, and β -Sb from zero-twist-angle 3×3 bilayer supercells by moving one of the two vdW layers in the two-dimensional plane and then inserting random perturbations less than 0.1 Å at each atomic site along x, y, and z directions. AB stacking adopts the same interlayer distance as AA stacking. Each dataset contains 576 shifted and perturbed supercell structures, respectively. The DFT Hamiltonians of these structures were calculated using the OpenMX with the Perdew–Burke–Ernzerhof (PBE) exchange–correlation function and the norm-conserving pseudopotentials.^{46–48} SOC was included in the band structure calculations. P7.0-s2p2d1, As7.0-s3p2d2, and Sb7.0-s3p2d2 pseudoatomic orbitals were used.⁴⁷ The calculated results were processed

by DeepH as datasets. The sizes of training, validation, and test sets are chosen as 346, 115, and 115, respectively. In the early stages of training, we use a larger learning rate to assist the model in quickly capturing global features of the data. As training progresses, the learning rate gradually decreases, allowing the model to converge better. The losses of β -P, β -As, and β -Sb on the best model validation set are 0.42, 0.51, and 0.40 meV, respectively (see Fig. S6 in the supplementary material).

First, we focus on the monolayer. Figures 1(a)–1(c) show the calculated band structure of monolayer β -P, β -As, and β -Sb. They are all semiconductors with indirect bandgaps. In addition, we also plot the projection weights of different atomic orbitals in this figure. It can be observed that for them, both the conduction band minimum (CBM) and valence band maximum (VBM) are mainly from the p orbital. Moreover, the states around the VBM near the Fermi level mainly from the contributions from p_z orbitals. This means that when forming their bilayers, the different stacking results in distinct interlayer coupling effects, which will lead to energy differences between VBM and CBM.

Next, we construct a bilayer of them. As shown in Fig. 2(a), there are two types of high-symmetry stacking structures, which are named AA and AB. Among the various bilayer stacking configurations, AA stacking has been established as the most stable structure,^{34,49,50} which is also focused here. The optimized parameters that include lattice constant (a), bond length (r), buckling height (h), and interlayer distance (d) are listed in Table I. We can find that a, r, and h are in good agreement with the previous study.^{31,33,49,50} However, the interlayer distance differs by ~6%,^{33,50–52} which can be sourced from the different methods used to treat vdW interaction. In this study, the DFT-D3 method with Becke Jonson damping is used, which is distinguished from the previous study. All three systems exhibit indirect bandgaps with values of 0.95, 0.60, and 0.56 eV, respectively, which is close to the values reported in the literature,^{32,34,49} as given in Table I.

For β -P and β -As, the band structures of bilayers with the AA and AB stackings are shown in Figs. 2(c) and 2(d). Referenced to the vacuum level, for β -P, we find the VBM energy in the AB stacking is $\Delta E \sim 0.26$ eV higher compared to that in the AA stacking. The ΔE for β -As and β -Sb are 0.36 eV [see Figs. 2(d)] and 0.20 eV (see S1 in the supplementary material). These values have significant importance, implying a large energy barrier for hole carriers when a

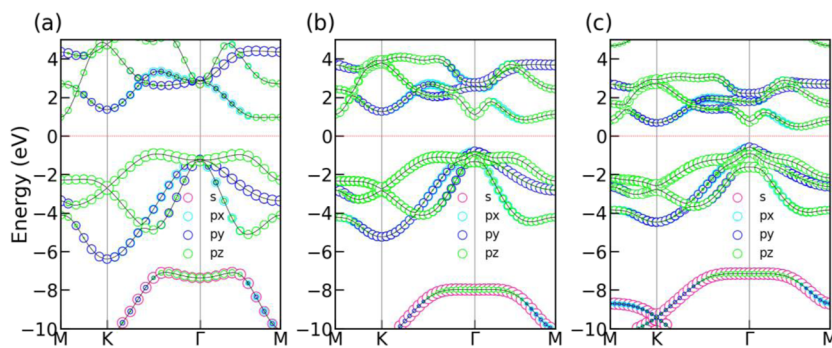


FIG. 1. Band structure of monolayer (a) β -P, (b) β -As, and (c) β -Sb. The contribution of s, p_x , p_y , and p_z orbitals is indicated by pink, cyan, blue, and green circles, respectively.

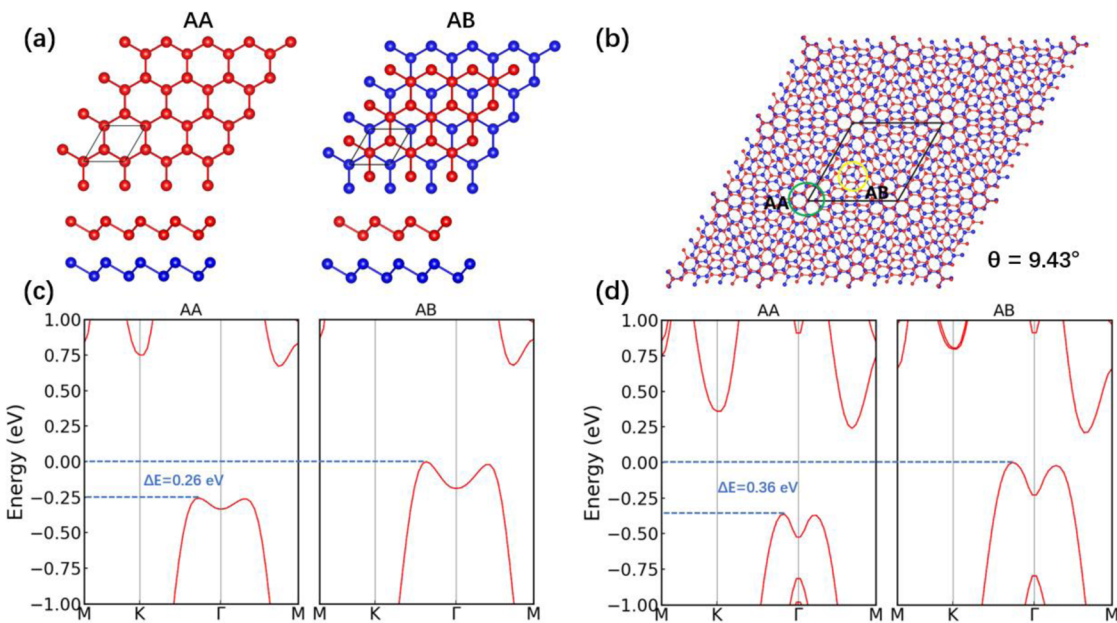


FIG. 2. (a) Top and side views of AA stacking and AB stacking. (b) Twisted bilayer of $\theta = 9.43^\circ$. The green and yellow circles highlight the AA stacking and AB stacking regions, respectively. Band structures of bilayer (c) β -P and (d) β -As with AA stacking and AB stacking, and the blue dashed lines indicate the height of VBM.

TABLE I. Structural parameters and bandgaps of AA stacked β -P, β -As, and β -Sb. The corresponding previous study values are provided in parentheses.

Crystal	a (Å)	r (Å)	h (Å)	d (Å)	E _g (eV)
β -P	3.25(3.28)	2.25(2.26)	1.24(1.24)	3.12(3.23)	0.93(0.98)
β -As	3.59(3.60)	2.50(2.51)	1.40(1.40)	2.95(3.14)	0.60(0.70)
β -Sb	4.08(4.10)	2.89(2.89)	1.66(1.67)	3.40(3.28)	0.56(0.49)

twisted bilayer material with these stackings is formed. This would limit the transition and conduction of electrons between neighboring sites because electrons need to overcome larger energy barriers (ΔE). The greater the ΔE , the larger the energy barrier that electrons must overcome. This could lead to a strong localization of electrons in the space between VBM or CBM and result in the isolation of flat bands around the Fermi level from other energy bands.⁵³ The system we are studying conforms to the new design principle proposed by Tao *et al.* to achieve ultra-flat bands in twisted 2D bilayers.⁵³ Specifically, monolayers and bilayers of β -P, β -As, and β -Sb exhibit semiconductor properties. Furthermore, in monolayers, the states around the VBM of them are dominated by p_z orbitals. Finally, there exists a large energy difference (ΔE) between their different stacking. Based on the above, ultra-flat bands are expected to exist at a large twist angle in their twisted systems.

In this study, we constructed 12 bilayer twisted structures for β -P, β -As, and β -Sb.⁵⁴ The number of atoms increases from 28 (21.8°) to 2524 (2.28°), which corresponds the supercell of $\sqrt{7} \times \sqrt{7} \times 1$ and $\sqrt{631} \times \sqrt{631} \times 1$. We selected the interlayer distance for AA stacking with the lowest energy to construct structures with different twist angles. We adopted a rigid stacking method

and did not perform structural relaxation on the twisted structure. Figure 2(b) shows the bilayer with a twist angle $\theta = 9.43^\circ$. The regions with local AA and AB stackings are marked with green and yellow circles, respectively.

The DFT data calculated by OpenMX are used to train three DeepH models for β -P, β -As, and β -Sb, respectively. To verify the accuracy of the models, we used OpenMX to calculate the band structures for twist angles of 21.78° , 13.17° , 9.43° , and 7.34° with 28, 76, 148, and 244 atoms, respectively (see S2 in the *supplementary material* for comparison of calculation time). Figure 3(a) shows the band structure computed by OpenMX (red lines) and predicted by DeepH (blue points) of β -As, where θ is the twist angle and N is the number of atoms. We found that the DeepH-trained models show an impressive level of agreement with the results calculated by OpenMX directly (see S3 and S4 in the *supplementary material* for β -P and β -Sb). We can find that at $\theta = 9.43^\circ$, a flat band appears below the Fermi level. Moreover, as the twist angle decreases, the bandgap gradually decreases, exhibiting a similar trend to previous studies.^{32,34} However, there are differences in the bandgap values, which may be due to the different DFT calculation methods used. For example, the bandgaps at 21.78° , 13.17° , 9.43° , and 7.34° for β -P are 1.05, 0.95, 0.91, and 0.85 eV, respectively. Whereas, previous studies reported values of 1.33, 1.18, 1.07, and 0.95 eV.³² For β -Sb, our calculated values are 0.71, 0.57, 0.50, and 0.45 eV (0.76, 0.58, 0.42, and 0.33 eV are the reported values in the literature).³⁴

To further investigate the relationship between twist angle and bandgap as well as flat bands, we continue to research smaller twist angles of 6.01° , 5.09° , 4.41° , 3.89° , 3.15° , 2.88° , 2.45° , and 2.28° . As shown in Fig. 3(b), the predicted band structures of twisted β -As with small twist angles by using DeepH (see S3 and S4 in the *supplementary material* for β -P and β -Sb) show that these materials

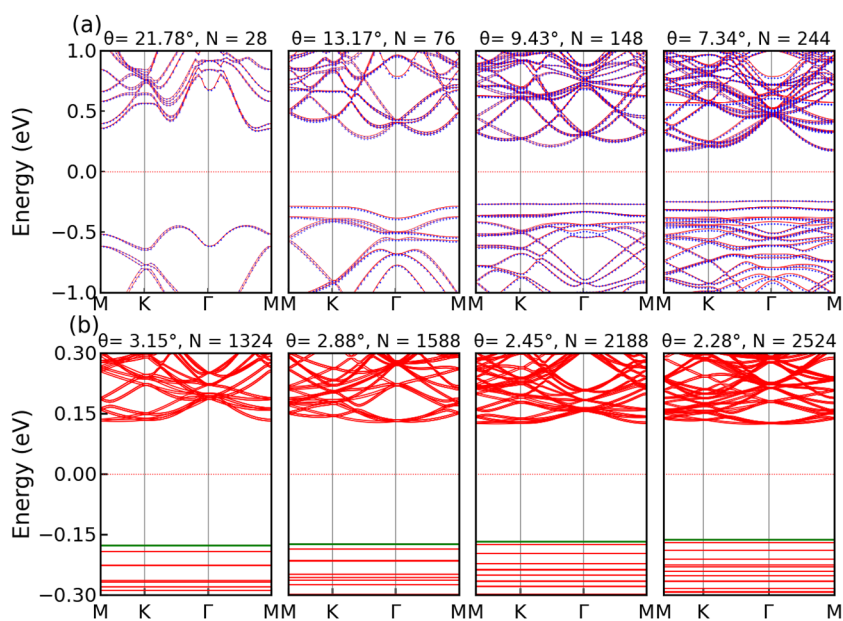


FIG. 3. (a) Comparison of OpenMX-calculated (red lines) and DeepH-predicted (blue points) energy band structures of twisted β -As with different twisted angles θ . (b) Energy band structures of twisted β -As with different twisted angles θ predicted by DeepH.

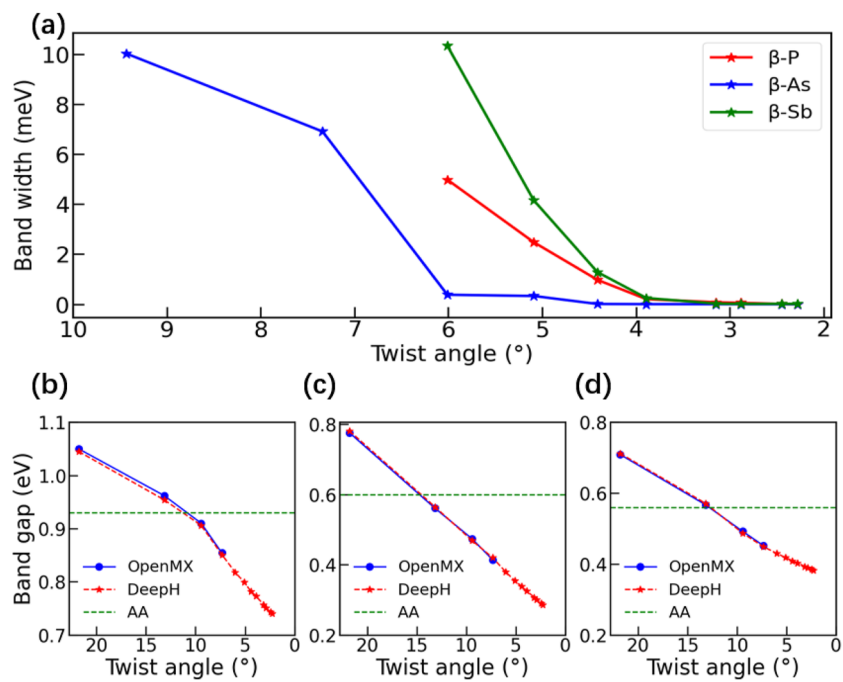


FIG. 4. (a) The variation of bandwidth with twist angle for β -P (red line), β -As (blue line), and β -Sb (green line). The variation of bandgap with twist angle for (b) β -P, (c) β -As, and (d) β -Sb.

exhibit similar properties at small twist angles. Specifically, numerous flat bands appear below the Fermi level, and the flat bands near the Fermi energy level are exceptionally flat, with each flat band being independent and well separated from others. However, the energy band of β -As begins to appear dispersion in the range of -0.4 to -0.3 eV (see S5 in the [supplementary material](#)). In addition, we found that as the twist angle decreases, the number of flat bands increases, and the first dispersion appears at lower energy levels. Our focus lies on the width of the first flat band below the Fermi level, represented by the green line.

It is interesting to note that as the twist angle decreases, flat bands start to show below the Fermi level in these three systems. Interestingly, in our study systems, the twisted bilayer of β -P, β -As, and β -Sb already exhibits significantly small bandwidths at the large twist angles, as shown in [Fig. 4\(a\)](#). Specifically, β -As exhibits a bandwidth of 10 meV at 9.43° , while β -P and β -Sb show bandwidths of 5 and 10 meV at 6.01° , respectively. More interestingly, the bandwidth of these three systems gradually decreases with the decrease in the twist angle and approaches 0 eV after 3.89° . So far, the appearance of ultra-flat bands in the available system requires delicate tuning to a very small twist angle. For example, a specific “magic angle” is needed to generate flat bands in graphene.^{4,5} For twisted bilayer MoS₂¹⁸ (hBN⁵⁵), the bandwidth of 23 meV (3 meV) only can be achieved at a 3.5° (2.28°) angle. Compared to them, we found the ultra-flat bands with a small bandwidth under a large twist angle. Moreover, the ultra-flat bands in β -P, β -As, and β -Sb can be formed over a wide range of angles, and the bandwidth decreases monotonically with the twist angles decreasing, which may lead to some exotic phenomena like twisted graphene. Our research provides a reference for the design of flat bands for twisted materials and provides a more versatile platform for the design of flat band devices.

To better illustrate the influence of twist angle on the bandgap, we present the variation of the bandgap with twist angle for the β -P, β -As, and β -Sb in [Figs. 4\(b\)–4\(d\)](#). To validate the predictions, we initially compared the bandgaps calculated by OpenMX with those predicted by DeepH for the first four twist angles. It can be found that the values closely agree with each other. Our research shows that their bandgap gradually decreases as the twist angle decreases, where the β -As display a larger slope. As the twist angles from 21.78° to 2.28° , the changes in the bandgap for β -P, β -As, and β -Sb are 0.305, 0.495, and 0.329 eV, respectively. Moreover, at 21.78° , the bandgaps of them are larger than the non-twisted structure. These findings show that their bandgaps are very sensitive to

changes in the twist angle, which provides a reference for the design and construction of group-V twisted bilayer materials with specific energy band structures and bandgaps.

Structural relaxation may have potential influences on the band structures. Taking β -As as an example, we evaluated the role of relaxation for twisted structures with more than 2000 atoms by using DeepMD-kit^{56,57} and calculated the band structure using DeepH. We have expanded the AA stacking of β -As into a $4 \times 4 \times 1$ supercell and performed *ab initio* molecular dynamics simulations using VASP at 300 K constant temperature for 10 000 steps. Through this process, we obtained a dataset of 10 000 frames, which was split into training and validation sets in an 8:2 ratio. The test performed on the validation set indicates that the mean absolute error (MAE) for each atomic energy and force was 10^{-4} eV and 0.01 eV/Å, respectively. Moreover, the convergence criterion of the Hellmann–Feynman force on each atom was less than 0.015 eV/Å. The bandwidth and bandgap of β -As at 9.43° optimized with DeepMD-Kit are 10.7 meV and 0.525 eV, respectively. There are only 0.9 meV and 0.004 eV different from the results of direct optimization using VASP (see Table S2 in the [supplementary material](#)). This indicates that the machine learning interatomic potentials we have constructed are accurate. As shown in [Fig. S12\(a\)](#) in the [supplementary material](#), the results indicate that structural relaxation increases bandgap, especially at small twist angles. The largest difference is about 0.14 eV. However, the effect of structural relaxation on bandwidth is relatively smaller. As shown in [Fig. S12\(b\)](#), a visible increase in the bandwidth can be found at large twist angles; however, the bandwidth is still smaller than the 12 meV, which corresponds to the value observed in twisted bilayer graphene at 1.08° . Moreover, as the twist angle decreases, the change in bandwidth converges to zero. For β -P and β -Sb, we also optimized the twisted structures at which flat bands begin to appear and compare the band structure with and without relaxation (see S9 and S11 in the [supplementary material](#)). The results are similar to the case of β -As. Therefore, our conclusion drawn from the rigid stacked structure is reasonable and relaxation has only slight effect on flat bands in group-V twisted bilayer materials.

It is well known that the electronic structure of two-dimensional materials can be affected by changes in interlayer distance. In our research, the DeepH model that we trained demonstrates strong generalization capabilities concerning interlayer distances as well. First, we investigated the bandgap changes of non-twisted β -P, β -As, and β -Sb under different interlayer distances, as shown in [Fig. 5\(a\)](#). We found that the bandgap increases with

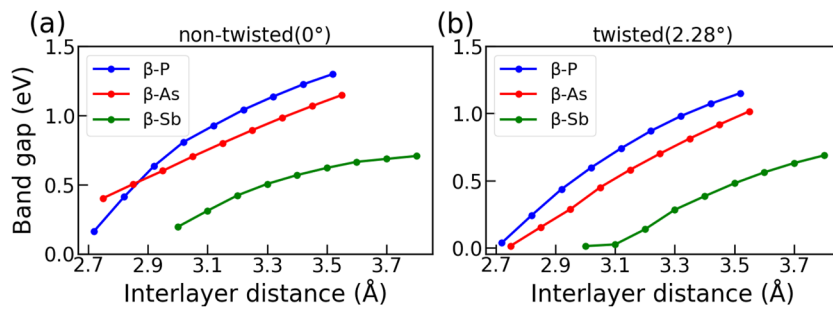


FIG. 5. The variation of β -P, β -As, and β -Sb bandgaps with interlayer distance: (a) non-twist angle of 0° and (b) twist angle of 2.28° .

increasing interlayer distances. Next, we investigated the effect of different interlayer distances on electronic structure at 2.28° (2524 atoms), as shown in Fig. 5(b). We found that by changing the interlayer distance, the flat band will remain while the bandgap will also increase with the increase in the interlayer distance. In addition, it is important to mention that the relationship between the bandgap of β -As and the interlayer distance is almost linear. Interestingly, β -P exhibits the highest slope at 2.28° . That is, as the interlayer distance increases, the bandgap of β -P increases fastest. Specifically, as the interlayer distance increases from 2.72 to 3.52 Å, the changes in the bandgap for β -P is 1.117 eV.

In this paper, we have investigated the twisted structures of β -phase P, As, and Sb by applying a deep learning approach. Our results show that the bandgap of the twisted structures of β -P, β -As, and β -Sb decreases with decreasing twist angle. In addition, as the interlayer distance increases, their bandgap also significantly increases. Interestingly, we found that flat bands appeared at a large twist angle, where β -As exhibits a flat band with a bandwidth of 10 meV at a twist angle of 9.43° . As the twist angle is further reduced, the bandwidth approaches 0 eV. This study provides an exceptional platform for investigating twisted bilayer 2D materials and exploring interesting phenomena associated with strongly correlated states.

The [supplementary material](#) includes the construction method of the twisted bilayer structures, the comparison of calculation time between DeepH and OpenMX, and the loss functions of the three models. In addition, the results show the energy band structures of twisted β -P and β -Sb with different twist angles. Finally, we have included the data on twisted β -Bi to provide a more complete investigation of group-V moirés material.

This work was supported by the National Natural Science Foundation of China (Grant No. 11874092), the Fok Ying-Tong Education Foundation, China (Grant No. 161005), and the Science Fund for Distinguished Young Scholars of Hunan Province (Grant No. 2021JJ10039).

AUTHOR DECLARATIONS

Conflict of Interest

The authors have no conflicts to disclose.

Author Contributions

Zhi-Xiong Que: Data curation (lead); Investigation (lead); Methodology (lead); Software (equal); Visualization (equal); Writing – original draft (equal); Writing – review & editing (equal). **Shu-Zong Li:** Data curation (equal); Formal analysis (equal); Investigation (equal); Methodology (equal); Visualization (equal). **Bo Huang:** Data curation (equal); Investigation (equal); Methodology (equal); Software (equal); Visualization (equal). **Zhi-Xiong Yang:** Conceptualization (supporting); Investigation (supporting); Supervision (supporting). **Wei-Bing Zhang:** Conceptualization (lead); Data curation (equal); Methodology (equal); Supervision (lead); Validation (equal); Writing – original draft (lead); Writing – review & editing (lead).

DATA AVAILABILITY

The data that support the findings of this study are available from the corresponding author upon reasonable request.

REFERENCES

- ¹J. S. Alden, A. W. Tsen, P. Y. Huang, R. Hovden, L. Brown, J. Park, D. A. Muller, and P. L. McEuen, "Strain solitons and topological defects in bilayer graphene," *Proc. Natl. Acad. Sci. U. S. A.* **110**(28), 11256–11260 (2013).
- ²C. R. Woods, L. Britnell, A. Eckmann, R. S. Ma, J. C. Lu, H. M. Guo, X. Lin, G. L. Yu, Y. Cao, R. V. Gorbachev, A. V. Kretinin, J. Park, L. A. Ponomarenko, M. I. Katsnelson, Y. N. Gornostyrev, K. Watanabe, T. Taniguchi, C. Casiraghi, H.-J. Gao, A. K. Geim, and K. S. Novoselov, "Commensurate-incommensurate transition in graphene on hexagonal boron nitride," *Nat. Phys.* **10**(6), 451–456 (2014).
- ³M. Yankowitz, J. Xue, D. Cormode, J. D. Sanchez-Yamagishi, K. Watanabe, T. Taniguchi, P. Jarillo-Herrero, P. Jacquod, and B. J. LeRoy, "Emergence of superlattice Dirac points in graphene on hexagonal boron nitride," *Nat. Phys.* **8**(5), 382–386 (2012).
- ⁴F. Wu and S. Das Sarma, "Collective excitations of quantum anomalous Hall ferromagnets in twisted bilayer graphene," *Phys. Rev. Lett.* **124**(4), 046403 (2020).
- ⁵M. Oh, K. P. Nuckolls, D. Wong, R. L. Lee, X. Liu, K. Watanabe, T. Taniguchi, and A. Yazdani, "Evidence for unconventional superconductivity in twisted bilayer graphene," *Nature* **600**(7888), 240–245 (2021).
- ⁶G. Shavit, E. Berg, A. Stern, and Y. Oreg, "Theory of correlated insulators and superconductivity in twisted bilayer graphene," *Phys. Rev. Lett.* **127**(24), 247703 (2021).
- ⁷S. Han, X. Nie, S. Gu, W. Liu, L. Chen, H. Ying, L. Wang, Z. Cheng, L. Zhao, and S. Chen, "Twist-angle-dependent thermal conduction in single-crystalline bilayer graphene," *Appl. Phys. Lett.* **118**(19), 193104 (2021).
- ⁸W. Ren, J. Chen, and G. Zhang, "Phonon physics in twisted two-dimensional materials," *Appl. Phys. Lett.* **121**(14), 140501 (2022).
- ⁹H. Li, S. Li, M. H. Naik, J. Xie, X. Li, J. Wang, E. Regan, D. Wang, W. Zhao, S. Zhao, S. Kahn, K. Yumigeta, M. Blei, T. Taniguchi, K. Watanabe, S. Tongay, A. Zettl, S. G. Louie, F. Wang, and M. F. Crommie, "Imaging moiré flat bands in three-dimensional reconstructed WSe₂/WS₂ superlattices," *Nat. Mater.* **20**(7), 945–950 (2021).
- ¹⁰Y. Cao, V. Fatemi, A. Demir, S. Fang, S. L. Tomarken, J. Y. Luo, J. D. Sanchez-Yamagishi, K. Watanabe, T. Taniguchi, E. Kaxiras, R. C. Ashoori, and P. Jarillo-Herrero, "Correlated insulator behaviour at half-filling in magic-angle graphene superlattices," *Nature* **556**(7699), 80–84 (2018).
- ¹¹Y. Cao, V. Fatemi, S. Fang, K. Watanabe, T. Taniguchi, E. Kaxiras, and P. Jarillo-Herrero, "Unconventional superconductivity in magic-angle graphene superlattices," *Nature* **556**(7699), 43–50 (2018).
- ¹²R. Bistritzer and A. H. MacDonald, "Moiré bands in twisted double-layer graphene," *Proc. Natl. Acad. Sci. U. S. A.* **108**(30), 12233–12237 (2011).
- ¹³B. L. Chittari, G. Chen, Y. Zhang, F. Wang, and J. Jung, "Gate-tunable topological flat bands in trilayer graphene boron-nitride moiré superlattices," *Phys. Rev. Lett.* **122**(1), 016401 (2019).
- ¹⁴F. Wu, T. Lovorn, E. Tutuc, I. Martin, and A. H. MacDonald, "Topological insulators in twisted transition metal dichalcogenide homobilayers," *Phys. Rev. Lett.* **122**(8), 086402 (2019).
- ¹⁵Y. Tang, L. Li, T. Li, Y. Xu, S. Liu, K. Barmak, K. Watanabe, T. Taniguchi, A. H. MacDonald, J. Shan, and K. F. Mak, "Simulation of Hubbard model physics in WSe₂/WS₂ moiré superlattices," *Nature* **579**(7799), 353–358 (2020).
- ¹⁶A. Ghiootto, E.-M. Shih, G. S. S. G. Pereira, D. A. Rhodes, B. Kim, J. Zang, A. J. Millis, K. Watanabe, T. Taniguchi, J. C. Hone, L. Wang, C. R. Dean, and A. N. Pasupathy, "Quantum criticality in twisted transition metal dichalcogenides," *Nature* **597**(7876), 345–349 (2021).
- ¹⁷Z. Zhang, Y. Wang, K. Watanabe, T. Taniguchi, K. Ueno, E. Tutuc, and B. J. LeRoy, "Flat bands in twisted bilayer transition metal dichalcogenides," *Nat. Phys.* **16**(11), 1093–1096 (2020).

- ¹⁸M. H. Naik and M. Jain, "Ultraflatbands and shear solitons in moiré patterns of twisted bilayer transition metal dichalcogenides," *Phys. Rev. Lett.* **121**(26), 266401 (2018).
- ¹⁹C. R. Woods, P. Ares, H. Nevison-Andrews, M. J. Holwill, R. Fabregas, F. Guinea, A. K. Geim, K. S. Novoselov, N. R. Walet, and L. Fumagalli, "Charge-polarized interfacial superlattices in marginally twisted hexagonal boron nitride," *Nat. Commun.* **12**(1), 347 (2021).
- ²⁰P. Kang, W.-T. Zhang, V. Michaud-Riou, X.-H. Kong, C. Hu, G.-H. Yu, and H. Guo, "Moiré impurities in twisted bilayer black phosphorus: Effects on the carrier mobility," *Phys. Rev. B* **96**(19), 195406 (2017).
- ²¹S. Zhang, S. Guo, Z. Chen, Y. Wang, H. Gao, J. Gómez-Herrero, P. Ares, F. Zamora, Z. Zhu, and H. Zeng, "Recent progress in 2D group-VA semiconductors: From theory to experiment," *Chem. Soc. Rev.* **47**(3), 982–1021 (2018).
- ²²M. Pumera and Z. Sofer, "2D monoelemental arsenene, antimonene, and bismuthene: Beyond black phosphorus," *Adv. Mater.* **29**(21), 1605299 (2017).
- ²³S. Zhang, M. Xie, F. Li, Z. Yan, Y. Li, E. Kan, W. Liu, Z. Chen, and H. Zeng, "Semiconducting group 15 monolayers: A broad range of band gaps and high carrier mobilities," *Angew. Chem., Int. Ed.* **55**(5), 1666–1669 (2016).
- ²⁴V. Tran, R. Soklaski, Y. Liang, and L. Yang, "Layer-controlled band gap and anisotropic excitons in few-layer black phosphorus," *Phys. Rev. B* **89**(23), 235319 (2014).
- ²⁵L. Li, Y. Yu, G. J. Ye, Q. Ge, X. Ou, H. Wu, D. Feng, X. H. Chen, and Y. Zhang, "Black phosphorus field-effect transistors," *Nat. Nanotechnol.* **9**(5), 372–377 (2014).
- ²⁶J. Qiao, X. Kong, Z.-X. Hu, F. Yang, and W. Ji, "High-mobility transport anisotropy and linear dichroism in few-layer black phosphorus," *Nat. Commun.* **5**(1), 4475 (2014).
- ²⁷S. Nahas, A. Bajaj, and S. Bhowmick, "Polymorphs of two dimensional phosphorus and arsenic: Insight from an evolutionary search," *Phys. Chem. Chem. Phys.* **19**(18), 11282–11288 (2017).
- ²⁸J. González and T. Stauber, "Kohn-Luttinger superconductivity in twisted bilayer graphene," *Phys. Rev. Lett.* **122**(2), 026801 (2019).
- ²⁹G. Tarnopolsky, A. J. Kruchkov, and A. Vishwanath, "Origin of magic angles in twisted bilayer graphene," *Phys. Rev. Lett.* **122**(10), 106405 (2019).
- ³⁰Y. W. Choi and H. J. Choi, "Strong electron-phonon coupling, electron-hole asymmetry, and nonadiabaticity in magic-angle twisted bilayer graphene," *Phys. Rev. B* **98**(24), 241412 (2018).
- ³¹S. Agnihotri, M. Kumar, Y. S. Chauhan, A. Agarwal, and S. Bhowmick, "Interlayer decoupling in twisted bilayers of β -phosphorus and arsenic: A computational study," *FlatChem* **16**, 100112 (2019).
- ³²D. A. Ospina, C. A. Duque, J. D. Correa, and E. Suárez Morell, "Twisted bilayer blue phosphorene: A direct band gap semiconductor," *Superlattices Microstruct.* **97**, 562–568 (2016).
- ³³A. C. R. Souza, M. J. S. Matos, and M. S. C. Mazzoni, "Interplay between structural deformations and flat band phenomenology in twisted bilayer antimonene," *RSC Adv.* **11**(45), 27855–27859 (2021).
- ³⁴Q. An, O. Moutanabbir, and H. Guo, "Moiré patterns of twisted bilayer antimonene and their structural and electronic transition," *Nanoscale* **13**(31), 13427–13436 (2021).
- ³⁵O. T. Unke, S. Chmiela, M. Gastegger, K. T. Schütt, H. E. Sauceda, and K.-R. Müller, "SpookyNet: Learning force fields with electronic degrees of freedom and nonlocal effects," *Nat. Commun.* **12**(1), 7273 (2021).
- ³⁶Q. Gu, L. Zhang, and J. Feng, "Neural network representation of electronic structure from *ab initio* molecular dynamics," *Sci. Bull.* **67**(1), 29–37 (2022).
- ³⁷H. Li, Z. Wang, N. Zou, M. Ye, R. Xu, X. Gong, W. Duan, and Y. Xu, "Deep-learning density functional theory Hamiltonian for efficient *ab initio* electronic-structure calculation," *Nat. Comput. Sci.* **2**(6), 367–377 (2022).
- ³⁸X. Gong, H. Li, N. Zou, R. Xu, W. Duan, and Y. Xu, "General framework for E(3)-equivariant neural network representation of density functional theory Hamiltonian," *Nat. Commun.* **14**(1), 2848 (2023).
- ³⁹V. Michaud-Riou, L. Zhang, and H. Guo, "RESCU: A real space electronic structure method," *J. Comput. Phys.* **307**, 593–613 (2016).
- ⁴⁰G. Kresse and J. Furthmüller, "Efficient iterative schemes for *ab initio* total-energy calculations using a plane-wave basis set," *Phys. Rev. B* **54**(16), 11169–11186 (1996).
- ⁴¹P. E. Blöchl, "Projector augmented-wave method," *Phys. Rev. B* **50**(24), 17953–17979 (1994).
- ⁴²G. Kresse and D. Joubert, "From ultrasoft pseudopotentials to the projector augmented-wave method," *Phys. Rev. B* **59**(3), 1758–1775 (1999).
- ⁴³J. P. Perdew, K. Burke, and M. Ernzerhof, "Generalized gradient approximation made simple," *Phys. Rev. Lett.* **77**(18), 3865–3868 (1996).
- ⁴⁴S. Grimme, J. Antony, S. Ehrlich, and H. Krieg, "A consistent and accurate *ab initio* parametrization of density functional dispersion correction (DFT-D) for the 94 elements H-Pu," *J. Chem. Phys.* **132**(15), 154104 (2010).
- ⁴⁵S. Grimme, S. Ehrlich, and L. Goerigk, "Effect of the damping function in dispersion corrected density functional theory," *J. Comput. Chem.* **32**(7), 1456–1465 (2011).
- ⁴⁶T. Ozaki, "Variationally optimized atomic orbitals for large-scale electronic structures," *Phys. Rev. B* **67**(15), 155108 (2003).
- ⁴⁷T. Ozaki and H. Kino, "Numerical atomic basis orbitals from H to Kr," *Phys. Rev. B* **69**(19), 195113 (2004).
- ⁴⁸I. Morrison, D. M. Bylander, and L. Kleinman, "Nonlocal Hermitian norm-conserving vanderbilt pseudopotential," *Phys. Rev. B* **47**(11), 6728–6731 (1993).
- ⁴⁹D. Kecik, E. Durgun, and S. Ciraci, "Stability of single-layer and multilayer arsenene and their mechanical and electronic properties," *Phys. Rev. B* **94**(20), 205409 (2016).
- ⁵⁰B. Ghosh, S. Nahas, S. Bhowmick, and A. Agarwal, "Electric field induced gap modification in ultrathin blue phosphorus," *Phys. Rev. B* **91**(11), 115433 (2015).
- ⁵¹Y. Kadioglu, J. A. Santana, H. D. Özaydin, F. Ersan, O. Ü. Aktürk, E. Aktürk, and F. A. Reboreda, "Diffusion quantum Monte Carlo and density functional calculations of the structural stability of bilayer arsenene," *J. Chem. Phys.* **148**(21), 214706 (2018).
- ⁵²Q. Xu, Y. Guo, and L. Xian, "Moiré flat bands in twisted 2D hexagonal vdW materials," *2D Mater.* **9**(1), 014005 (2021).
- ⁵³S. Tao, X. Zhang, J. Zhu, P. He, S. A. Yang, Y. Lu, and S.-H. Wei, "Designing ultra-flat bands in twisted bilayer materials at large twist angles: Theory and application to two-dimensional indium selenide," *J. Am. Chem. Soc.* **144**(9), 3949–3956 (2022).
- ⁵⁴J. M. B. Lopes dos Santos, N. M. R. Peres, and A. H. Castro Neto, "Graphene bilayer with a twist: Electronic structure," *Phys. Rev. Lett.* **99**(25), 256802 (2007).
- ⁵⁵X.-J. Zhao, Y. Yang, D.-B. Zhang, and S.-H. Wei, "Formation of Bloch flat bands in polar twisted bilayers without magic angles," *Phys. Rev. Lett.* **124**(8), 086401 (2020).
- ⁵⁶J. Zeng, D. Zhang, D. Lu *et al.*, "DeePMD-kit v2: A software package for deep potential models," *J. Chem. Phys.* **159**(5), 054801 (2023).
- ⁵⁷H. Wang, L. Zhang, J. Han, and W. E, "DeePMD-kit: A deep learning package for many-body potential energy representation and molecular dynamics," *Comput. Phys. Commun.* **228**, 178–184 (2018).